

Electrochemical synthesis of poly(2-methyl aniline): electrochemical and spectroscopic characterization

ALEKSANDRA BUZAROVSKA, IRENA ARSOVA and LJUBOMIR ARSOV*

Faculty of Technology and Metallurgy, University "St. Cyril and Methodius", 91000 Skopje, Macedonia

(Received 21 June, revised 31 October 2000)

Poly(2-methyl aniline) or poly(*ortho*-toluidine), as ring substituted derivative of aniline, has been synthesized electrochemically in various concentrations of H₂SO₄ and HCl, and then characterized by cyclic voltammetry, as well as by impedance and Raman spectroscopy. The cyclic voltammograms of poly(*o*-toluidine) and poly(aniline) show that the electrochemical polymerization of these two polymers proceeds by almost identical mechanisms. The Raman spectroscopical measurements suggest that the redox reactions of poly(aniline) and poly(*o*-toluidine) are similar in the potential range between –0.2 and 0.7 V *vs.* SCE. The impedance measurements showed that the conductivity of poly(*o*-toluidine) is an order of magnitude lower than that of the corresponding poly(aniline) form.

Keywords: poly(2-methyl aniline), electropolymerization, cyclic voltammetry, Raman spectroscopy.

INTRODUCTION

In the last twenty years great scientific attention has been paid to electroconductive polymers such as: poly(acetylene)s, poly(thiophene)s, poly(pyrrole)s, poly(aniline)s, *etc.* Among all these polymers particular interest has been paid to poly(aniline) (PANi) due to its high conductivity in the oxidized state, low weight and environmental stability. One of the most useful methods for the preparation of PANi and its ring substituted derivatives is electrochemical synthesis.^{1–3} Electrochemical synthesis is usually carried out by cyclic voltammetry with the cathodic potential in the range between –0.2 V and 0 V *vs.* SCE and the anodic potential in the range between 0.7 V and 1.2 V *vs.* SCE in acidic aqueous solutions containing monomer.^{4–6} The polymeric material is deposited on the working electrode, and its redox state can be well controlled by the value of the applied potential. So far, most of the studies have been devoted to the polymerization mechanism of PANi, and also to the influence of the pH value, the nature of supporting electrolyte, anion effects, monomer concentration, *etc.*^{7–10}

The large-scale application of PANi is sometimes limited by the insolubility of its protonated state and the difficulty of processing by conventional methods. This short-

* Author for correspondence, tel. ++389(91)362-031, fax: ++389(91)365-389, E-mail: arsov@ukim.edu.mk.

coming has usually been overcome by preparing PANi films in functionalised acids,^{11,12} or by the synthesis of various PANi copolymers,^{13,14} as well as the polymerization of different alkyl-ring substituted monomers. Whereas many reports deal with the electrochemical synthesis and properties of aniline derivatives, much less is known about their polymerization mechanism.

In this paper, the main efforts will be focused on the electrochemical synthesis of poly(*o*-toluidine) and its characterization using cyclic voltammetry, impedance and Raman spectroscopy. The structure and the redox reactions of poly(*o*-toluidine) films will be compared with the already well known structure and redox reactions of PANi films, published in our previous papers.^{15,16}

EXPERIMENTAL

Prior to the electrochemical polymerization, *o*-toluidine was purified by vacuum distillation. Poly(*o*-toluidine) films (POT) were synthesized in aqueous solutions of H₂SO₄ and HCl of varying molarity (0.5 M, 1 M and 2 M acid concentrations were used). Different concentrations of *o*-toluidine in the corresponding electrolytes were employed. For the cyclic voltammetric measurements, a three-cell electrode system (similar to the earlier procedure) was used.¹⁷ The POT films were grown on a Pt working electrode (78 mm²), by cycling the potential between -0.2 V and 1.2 V, as well as -0.2 V and 0.7 V vs. SCE. An alternative approach was also applied: namely, the first two cycles were scanned with the very low sweep rates of 2 mV s⁻¹ in the range from -0.2 to 1.2 V vs. SCE, and then the next cycles were scanned at different rates, *i.e.*, 20, 50 or 100 mV s⁻¹, in the same or reduced anodic potential up to 0.7 V, and 0.8 V vs. SCE. Prior to each run, the Pt electrode was polished with 0.1 μm diamond paste and ultrasonically washed with methanol and distilled water. A Pt foil was used as the counter electrode, and a saturated calomel electrode (SCE) as the reference electrode. All potentials in this work are referred to the saturated calomel electrode (SCE). The solutions were degassed in the electrochemical cell by bubbling argon through them for at least 30 min. After the electrochemical polymerization, the films were washed with distilled water in order to remove the low molecular soluble products.

The cyclic voltammetry measurements were performed using a HEKA Model 488 potentiostat-galvanostat interfaced with personal computer. The Raman spectra were recorded using a Phillips instrument in the spectral range between 100 cm⁻¹ and 1800 cm⁻¹. The 632.8 nm excitation line of a 100 mW He/Ne laser was used. The conductivity measurements were performed in a three-cell IM5d impedance measurement system "Zahner electric".

RESULTS

Cyclic voltammetry (CV)

The electrochemically prepared POT and PANi give identical cyclic voltammograms under the same experimental conditions. The initial CV curve shows an irreversible oxidation peak between 0.8 V and 1 V (depending on the scan rate).¹ After several cycles this peak disappears and the newly formed redox anodic and cathodic peaks increase in intensity in each next cycle.

The cyclic voltammograms for two different concentration of H₂SO₄ containing 0.1 M *o*-toluidine are shown in Fig. 1.

It is evident that the shapes of the voltammograms are quite different, depending on the concentration of the supporting electrolyte. In Fig. 1a, intensive anodic and cathodic peaks are observed at 0.43 V and 0.33 V, respectively, with almost invisible shoulders. These two peaks are mainly due to the degradation of the polymer and soluble sur-

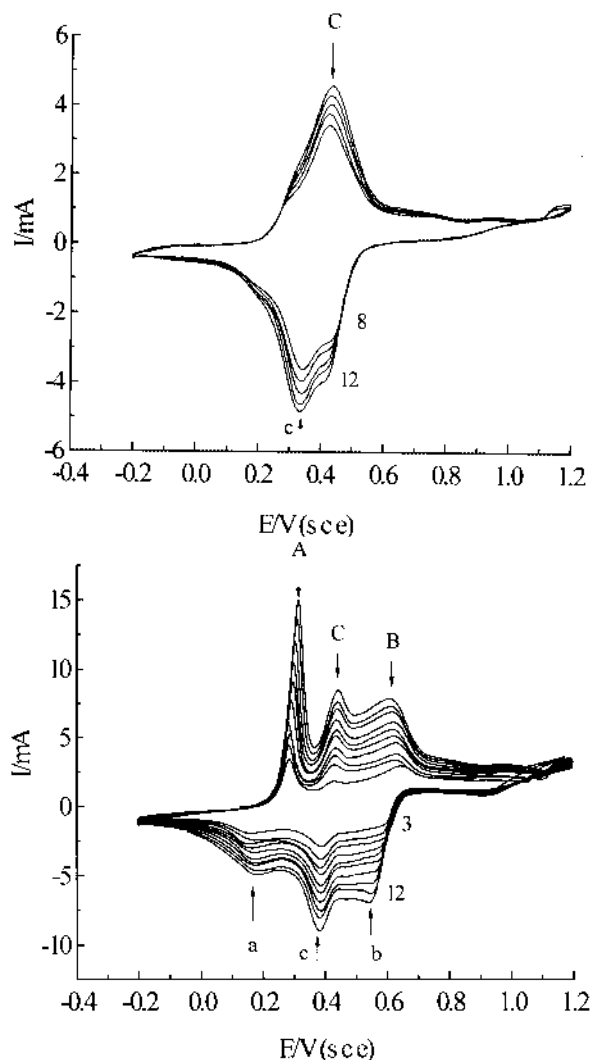


Fig. 1. a) Cyclic voltammogram of POT formation on a Pt electrode in aqueous 0.5 M H₂SO₄ + 0.1 M o-toluidine solution ($\nu = 20$ mV/s); potential range between -0.2 to +1.2 V vs. SCE. The numbers 8 and 12 indicate the 8th and 12th cycle. b) Cyclic voltammogram on a Pt electrode in aqueous 2 M H₂SO₄ + 0.1 M o-toluidine solution ($\nu = 20$ mV/s); potential range between -0.2 to +1.2 V vs. SCE. The numbers 3 and 12 indicate the 3rd and the 12th cycles after the first two cycles scanned at the low sweep rate of 2 mV/s.

face-bound products.¹⁸ At the same time, during the cycling, the electrode is covered with a thick deposit and extensive dissolution occurs. The solution near the electrode surface became an intensive green colour. For lower anodic potential limits, (up to 0.7 V), the voltammograms showed only poor, undefined large peaks.

In the higher H₂SO₄ concentration (Fig. 1b), three redox peaks are detectable and the voltammograms show similar shapes as in the case for PANi.¹⁵ It can be said that the identical redox process occurs during cycling of these two polymers.

For a reduced anodic potential limit (up to 0.8 V), (Fig. 2) and higher concentration of added monomer, the shapes of the voltammogram are almost identical with those reported by Cattarin *et al.*¹⁹

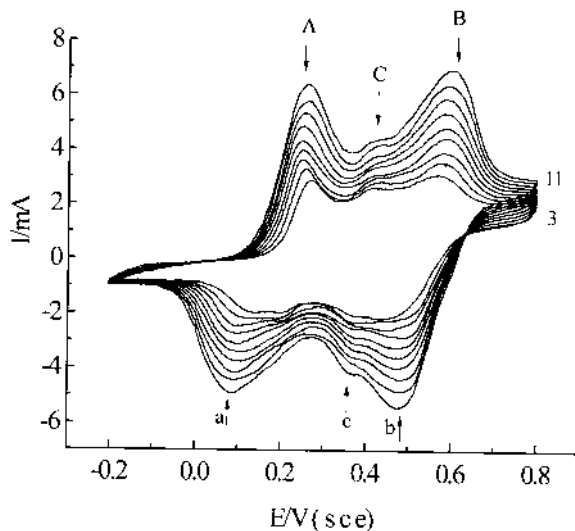


Fig. 2. Cyclic voltammograms of POT film obtained in 2 M H_2SO_4 + 0.3 M *o*-toluidine solution ($\nu = 20$ mV/s); potential range between -0.2 and $+0.8$ V vs. SCE. Numbers 3 and 11 indicate the 3rd and 11th cycle after the first two cycles scanned at the low sweep rate of 2 mV/s in the range between -0.2 V and 1.2 V vs. SCE.

Two pairs of well resolved redox peaks A/a and B/b which progressively develop at 0.25 V and 0.6 V can be seen in Fig. 2. This strongly resembles the behaviour of PANi. Only a third pair of redox peaks, the so called “middle peaks” C/c, which belong to the degradation products²⁰ is poorly recognized. As expected, due to the presence of the electron-releasing methyl group in the *ortho*-position, the potentials of the first peaks A/a in POT are slightly less positive than the corresponding values in PANi.

A comparison of Fig. 1 and Fig. 2 shows that the regular oxidative voltammetric behaviour of *o*-toluidine is possible only in higher concentrations of H_2SO_4 and *o*-toluidine.

The cyclic voltammograms for POT films grown in HCl, with a reduced anodic potential limit (up to 0.7 V) are presented of Fig. 3.

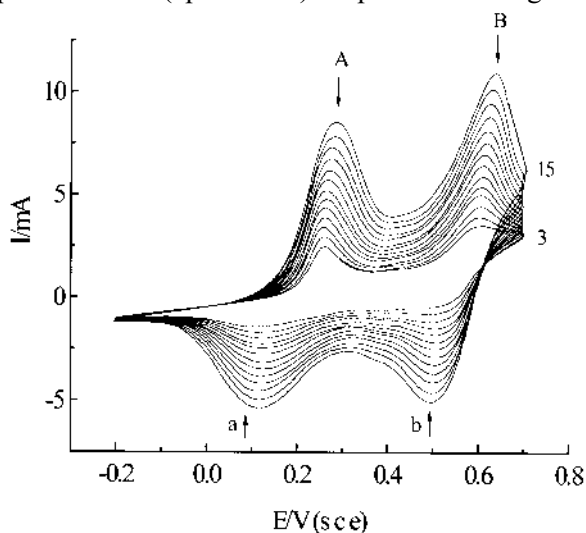


Fig. 3. Cyclic voltammograms of POT electropolymerized in 2 M HCl + 1 M *o*-toluidine solution ($\nu = 20$ mV/s); potential range between -0.2 to $+0.7$ V vs. SCE. Numbers 3 and 15 indicate the 3rd and the 15th cycle.

It should be noted that, compared to H_2SO_4 , higher acid (2 M HCl) and monomer (> 0.5 M *o*-toluidine) concentration were required in order to obtain a reasonable polymer growth. In agreement to previously reported results,¹⁶ for 1 M HCl and 0.1 M *o*-toluidine, very poor voltammograms with already inactive peaks were registered.

Two pairs of redox peaks were detected without any potential shift. No middle peaks C/c were detected, confirming the non-existence of degradation products and higher regularity, homogeneity and adherence of the deposited film to the electrode surface, than in the case of polymer deposited from H_2SO_4 solutions.

With the same electrochemical conditions, the curve shapes of POT almost replicate the electrochemical behaviour of PANi,^{15,22} confirming once more that the mechanism of the redox processes in POT are the same as in the case of PANi.

Impedance measurements

Only qualitative impedance measurements were performed, in order to estimate the conductivity of the POT films for various applied cyclic voltammetry potentials. The Bode diagrams of the POT film prepared in HCl for the forward and reverse cycles at two fixed potentials of 0.7 V and 0.3 V are shown in Fig. 4.

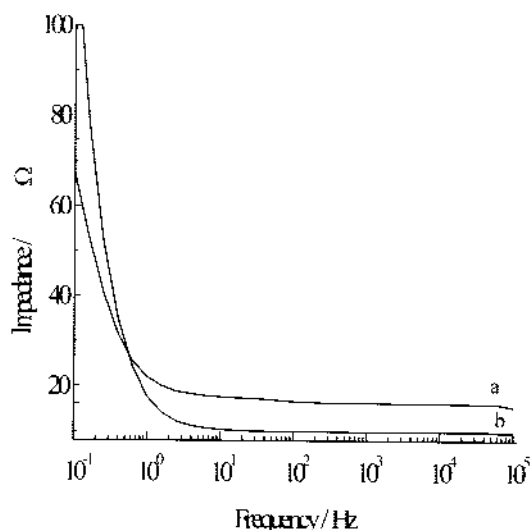


Fig. 4. Bode plots of POT films in 2 M HCl: a) anodic sweep at fixed potential of 0.7 V vs. SCE; b) reverse sweep at a fixed potential of 0.3 V vs. SCE.

It is evident that in the higher frequency region, the impedance values are very low, reaching almost negligible values (below 10 ohms). The impedance curves exhibit similar shapes as in the case of PANi.²² The results suggest that the POT films prepared in HCl solutions have high conductivity, but lower than that of PANi,²³ under the same experimental conditions. The conductivities of PANi and POT were found to be 5 S cm^{-1} and $1 \cdot 10^{-1} \text{ S cm}^{-1}$, respectively. It is not quite clear how the *ortho* substituted electron donating methyl group modifies the conductivity of the polymer. However, besides the chemical structure and chain conformation, there are many factors that may influence the conductivity, such as chain packing and morphology of the polymer. The methyl group of the phenyl ring in the *o*-toluidine can be expected to increase the tor-

sional angle between adjacent rings to relieve the steric strain. This may contribute to the lower conductivities of POT as compared to the unsubstituted PANi.

The results of impedance measurements obtained in H_2SO_4 are not shown, since the POT films in H_2SO_4 solutions free of monomer, were not very stable during the potential cycling.

Further theoretical and experimental work is necessary to evaluate the contributions of various factors to the conductivity of POT.

Raman spectroscopy

The Raman spectra of PANi and POT in oxidized form, under potentiostatic conditions, at a fixed potential of 0.7 V are shown in Fig. 5.

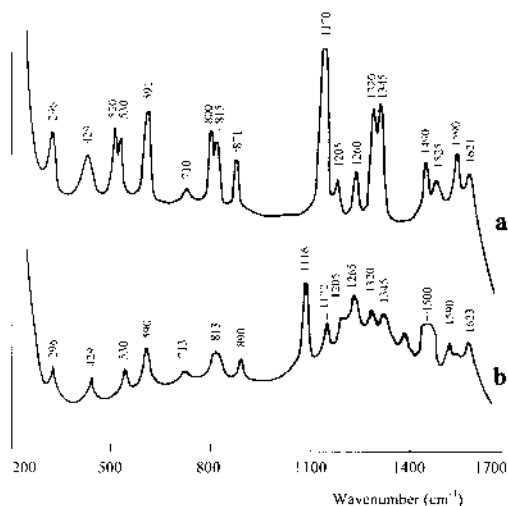


Fig. 5. *In-situ* Raman spectra recorded at a fixed potential of 0.7 V vs. SCE: a) PANi; b) POT.

The electrolyte background was subtracted from the measured spectra and only the spectra resulting from the PANi and POT films are presented.

The assignments of the Raman bands are listed in Table I.

Comparing these two spectra, big differences in intensity of spectral bands are observed. Namely, all the spectral bands of POT have considerably lower intensities than those of PANi and some of them are poorly defined. This effect is probably due to the larger thickness of the deposited POT film on the electrode surface and the higher absorption of the scattered Raman light in them. A small fluorescence effect is also observed.

The most dominant band in the POT spectrum is located at 1116 cm^{-1} . This band can be attributed to the $(\text{C}-\text{C})$ vibration in the methyl substituted semiquinone and quinone rings and does not exist in the PANi spectrum. The most dominant band in the PANi spectrum is located at 1170 cm^{-1} . This band can be attributed to the $\text{C}-\text{H}$ vibration in the plain bending mode of the semiquinoid radical cation (polaron and quinoid rings). Taking into account that the structures of the polarons and quinoid rings are not

stable but relax into semiquinone radical cations, according to the polaron lattice theory, the band at 1170 cm^{-1} is assigned to the semiquinone radical cation. The small difference of the wave number of this band between PANi and POT is due to the methyl group attached to the benzene ring.

TABLE I. Raman frequencies in the range between $100\text{--}1800\text{ cm}^{-1}$ for POT and PANi at a potential of 0.7 V vs. SCE . Exciting wave 632.8 nm

Frequencies		Raman assignments	Wilson notation*
PANi	POT		
296 <i>m</i>	296 <i>m</i>	(C-N) in SQ and Q	
429 <i>m</i>	429 <i>m</i>	(C-N) in SQ and Q	
520 <i>s</i>	530 <i>m</i>	(C-C) in SQ and Q	16 b
530 <i>s</i>			
591 <i>s</i>	590 <i>m</i>	(C-C) in B	6a
710 <i>m</i>	713 <i>m</i>	(C-C) in <i>p</i> -disubstituted B ring	4
800 <i>s</i>	813 <i>m</i>	(C-C) in B	1
815 <i>s</i>			
871 <i>m</i>	890 <i>m</i>	(C-H) in B and Q	10a
	1116 <i>s</i>	(C-C) in methyl substituted SQ and Q rings	
1170 <i>s</i>	1172 <i>m</i>	(C-H) in SQ	9a
1205 <i>m</i>	1205 <i>sh</i>	(C-N) in B ring	
1260 <i>m</i>	1265 <i>m</i>	(C-N) in SQ and Q	
1320 <i>s</i>	1320 <i>w</i>	(C-N) + (C-C) in B	
1345 <i>s</i>	1345 <i>w</i>	polaronic part	
1490 <i>m</i>	1500 <i>m</i>	(C=N) head to tail polymerization	
1525 <i>w</i>	1525 <i>ch</i>	In SQ and Q rings	
1590 <i>m</i>	1590 <i>sh</i>	(C=C) in B, SQ and Q	8b
1621 <i>m</i>	1623 <i>m</i>	(C=C) in B	8b

s: strong, *sh*: shoulder, *m*: medium, *w*: weak; B: benzoic ring, SQ: semiquinoid ring and Q: quinonid ring. * Assignments are given using the Wilson notation for the vibrational spectra of benzene derivatives (G. Varsanyi, assignments for vibrational spectra of benzene derivatives, Vol. 1, Adams Hilger, London, 1987)

Strong Raman bands, which are the main bands of the semiquinone radical cation appear at 1323 cm^{-1} and 1341 cm^{-1} . These two bands arise from (C-C) and (C-N) vibrations in the benzene ring. Periera *et al.*,²⁴ observed only one band at 1333 cm^{-1} , said to be an indication of the presence of quinoid segments, while the conversion of quinoic rings into benzene rings was followed by increase in the intensity of the band.

The bands located at 1490 cm^{-1} and 1525 cm^{-1} in spectra of PANi are characteristic for head to tail coupling and arise from $(\text{C}=\text{N})$ vibration in the polymer chain. However, these two bands are ill separated in the spectra of POT and merge into one large band. The bands located at: 830 cm^{-1} , 883 cm^{-1} and 1625 cm^{-1} are characteristic for *p*-disubstituted benzene rings.

DISCUSSION

In aqueous acid electrolytes, poly(*o*-toluidine) can be easily synthesized by cyclic voltammetry in the potential range between -0.2 and 0.7 V . However, no polymer is deposited on the electrode surface in the above mentioned potential region during the first scan. The recommended anodic potential limit for the first few scans is 1.2 V .

The initiation of polymer nucleation and its skeleton formation occurs above 0.9 V . The number of nuclei strongly depends on the prepolarization conditions. After several cycles, the anodic potential limit must be reduced from 1.2 V to at least to 0.7 V in the order to eliminate the formation of degradation products during the film growth.²⁰ It can be concluded that *o*-toluidine must be in some oxidized state to initiate polymer nucleation (in the first two cycles). The oxide species of *o*-toluidine autocatalize the polymer growth, therefore, it is not necessary to cycle the potential in the anodic sweep above 0.7 V .

The voltammetric results and the quality of the electrodeposited films suggest that the nature and concentration of the acid, as well as the monomer concentration, play a big role in the formation of the polymer structure.

In lower concentrations of H_2SO_4 (Fig. 1a), a rapid increase of a pair of large broad waves, which could be assumed to be the “middle peaks” occurs.²¹ These middle peaks have been attributed to the oxidation/reduction of degradation products. Spectroscopic data confirmed the presence of degradation products (benzoquinone type compounds)¹⁵ as precipitates in the polymer film. Due to the degradation products, the adherence of the electrodeposited film is poor and it peels off from the electrode surface.

At higher concentrations of H_2SO_4 (Fig. 1b), three pairs of well resolved redox peaks were detected. The peaks A/a and B/b belong to the electroactive switching reactions in POT, while the peaks C/c belong to the degradation products. The presence of degradation products diminishes the electroactivity of the polymer film and its adhesion to the electrode surface. In this case, during cycling, the diffusion of soluble colored degradation products from the electrode surface into the bulk electrolyte was obvious.

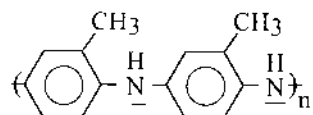
In our earlier reports, it was shown that the degradation products in PANi films consist of: *p*-benzoquinone, hydroquinone, *p*-aminophenol, and quinoneimine.¹⁵ Some authors believe that the middle peaks are closely related to the cross-linking reactions, giving a two dimensional polymer with phenazine rings,²⁵ and also to *ortho* or *meta* coupling.²⁶

In this study the presence of phenazine structure could hardly be assumed. Raman spectroscopic measurements gave no evidence of the characteristic bands for cross-linking reactions. The possibility of *ortho*-coupling in POT should be taken with a great reserve, as one of the *ortho* positions in *o*-toluidine is blocked with a methyl group.

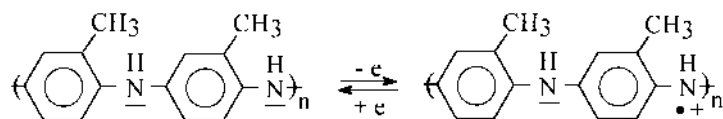
The most regular electrodeposition were obtained in aqueous solutions containing 2 M HCl and 0.3 M *o*-toluidine. The cycling was carried out in the potential range between -0.2 V and 0.7 V (Fig. 3). Only two pairs of well defined peaks A/a and B/b gradually formed and the electrodeposited film adhered well to the electrode surface. There was no evidence of the middle peaks on the voltammogram and also no visible diffusion of soluble colored products from the electrode surface to the bulk electrolyte, during cycling. The regular increase in the current with each cycle indicates a regular growth of the film thickness. The potential position of the redox peaks does not shift with increasing number of cycles, indicating that the reversibility of the redox reactions is independent of film thickness. The electroactivity and switching reactions in the polymer film were reversible and with each cycle the color of the electrodeposited film changed alternatively from pale yellow at -0.2 V to green at 0.4 V and then to blue and violet at 0.7 V. The potential difference between first and second redox process for PANi in 2 M HCl is 0.6 V. For POT this difference is significantly lower (0.4 V). In comparison to PANi, the potential for the first redox process is higher for POT and lower for the second one. This indicates that the electroactivity of POT occurs in a shorter potential region than the electroactivity of PANi.

Comparing the voltammograms and the Raman spectra of PANi and POT, the structure and redox reactions in POT, for various applied potentials, can be postulated. The Raman spectra show the existence of *p*-disubstituted benzene rings, as well as semiquinones and quinones rings.

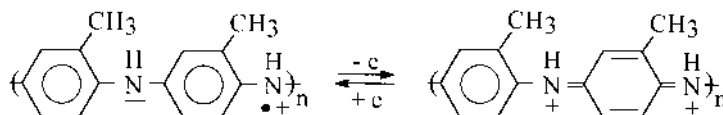
Analogues with aniline, radical cations of *o*-toluidine are formed, in the first positive scan, leading to the formation of dimer products adsorbed on the electrode surface. These dimer products react with the monomer units of *o*-toluidine and form polymerized segments of:



The first redox waves A/a correspond to the removal of electrons from the nitrogen atoms of the amine between the benzene rings, *i.e.* conversion of amine units to radical cations (semiquinones):



The second redox waves B/b can be assigned to the oxidation/reduction of the semiquinone radical cation (polarone state) to quinone imine (bipolarone state), verified by Raman bands at 1261 cm^{-1} , 1478 cm^{-1} and 1518 cm^{-1} :



Therefore, the second redox process is attributed to the conversion of radical cations to the fully oxidized form (quinoidal structure).

From the Raman spectra, it is evident that the electropolymerization and redox reactions in POT film proceed by head-to-tail coupling. A Raman band, located at 1404 cm^{-1} , characteristic for N=N stretching vibrations, is not observed. This indicates that there is no head-to-head coupling in the polymer chain. The polymer chain consists mainly of *para*-coupling of semiquinone, quinone and benzene rings, in the ratio depending on the applied potential.

CONCLUSIONS

The following conclusions can be drawn from the voltammetric, impedance and *in-situ* Raman spectroscopical measurements:

– Potentiodynamic electrosynthesis of poly(*o*-toluidine) in H_2SO_4 and HCl, for potential range between -0.2 V and 0.7 V vs. SCE , leads to the formation of uniform and electroactive films. For regular film thickness growth on the electrode surface, during cycling, the concentration of *o*-toluidine in the supporting electrolyte must be at least five times higher in HCl than in H_2SO_4 .

– The cyclic voltammograms consist of two pairs of well-resolved redox peaks, the first corresponding to the conversion of amine nitrogens to radical cations, and the second to the conversion of the radical cations to imine nitrogens.

– The conductivity of POT is about an order of magnitude lower than the conductivity of PANi. The steric effects of the alkyl-substituent (POT) are probably responsible for the decrease in its conductivity.

– The Raman measurements show that PANi and POT, prepared under identical experimental conditions have similar spectra. The existence of *para*-disubstituted benzene rings, semiquinoid radical cations and quinoid rings in the polymer chain are suggested, by the Raman assignment.

– Finally, the voltammetric and Raman spectroscopical measurements showed identical mechanism of electropolymerization, as well as redox processes in the PANi and POT films.

Acknowledgment: We thank the Ministry of Science of the Republic of Macedonia for their financial support of this work.

ИЗВОД

ЕЛЕКТРОХЕМИЈСКА СИНТЕЗА ПОЛИ(2-МЕТИЛ АНИЛИНА): ЕЛЕКТРОХЕМИЈСКА И СПЕКТРОСКОПСКА КАРАКТЕРИЗАЦИЈА

АЛЕКСАНДРА БУЗАРОВСКА, ИРЕНА АРСОВА и ЛЈУБОМИР АРСОВ

Технолошко-металуршки факултет, Универзитет "Кирил и Методиј" Скопје, Македонија

Поли(2-метил анилин), као супституован дериват анилина, синтетизован је електрохемијским путем на Pt електроди у растворима сумпорне и хлороводоничне киселине. Карактеризација је изведена цикличном волтаметријом, импедансном и Рамановом спектроскопијом. Упоређивањем цикличног волтаметријског понашања поли(2-метил ани-

лина) и поли(анилина), предложен је идентичан механизам електрохемијске полимеризације. На основу Раман спектроскопских мерења, предложене су сличне редокс реакције у потенцијалном подручју између $-0,2$ и $0,7$ V vs. (ЗКЕ). Импедансна мерења су показала да је проводљивост поли(2-метил анилина) за цео ред величине нижа од оне код полианилина.

(Примљено 21. јуна, ревидирано 31. октобра 2000)

REFERENCES

1. A. Efremova, A. Regis, Lj. Arsov, *Electrochim. Acta* **39** (1994) 839
2. G. Tourillon, F. Garnier, *J. Electroanal. Chem.* **135** (1982) 173
3. W. Focke, G. Wnek, Y. Wei, *J. Phys. Chem.* **91** (1988) 173
4. Lj. Arsov, *J. Solid State Electrochem.* **2** (1998) 266
5. D. Stillwel, S. M. Park, *J. Electrochem. Soc.* **135** (1988) 2254
6. A. Efremova, Lj. Arsov, *J. Serb. Chem. Soc.* **57** (1992) 127
7. W-S. Huang, B. D. Humphrey, A. G. MacDiarmid, *J. Chem. Soc., Faraday Trans. 1*, **82** (1986) 2385
8. E. M. Genies, J. F. Penneau, E. Vieil, *J. Electroanal. Chem.* **283** (1990) 205
9. N. Oyama, Y. Ohnuki, K. Chiba, T. Ohsaka, *Chem. Lett.* (1983) 1759
10. R. Noufi, A. J. Nozik, J. White, L. Fwarren, *J. Electrochem. Soc.* **129** (1982) 2261
11. S. J. Davies, T. G. Ryan, C. J. Wilde, G. Beyer, *Synth. Met.* **69** (1995) 209
12. T. Vikki, O. T. Ikkala, *Synth. Met.* **69** (1995) 235
13. M. Sato, S. Yamanaka, J. Nakaya, K. Hyodo, *Electrochim. Acta* **39** (1994) 2159
14. J. J. Langer, *Synth. Met.* **35** (1990) 301
15. Lj. Arsov, W. Plieth, G. Kobmehl, *J. Solid State Electrochem.* **2** (1998) 335
16. Lj. Arsov, K. Colanceska, N. Petrovska, *J. Serb. Chem. Soc.* **63** (1998) 289
17. Lj. Arsov, C. Kormann, W. Plieth, *J. Raman Spectroscopy* **22** (1991) 573
18. E. Genies, Panneau, M. Lapkowski, *New J. Chem.* **12** (1988) 46
19. S. Cattarin, L. Doubova, G. Mengoli, G. Zotti, *Electrochim. Acta* **33** (1988) 1077
20. M. Leclerc, J. Guay, L. H. Dao, *J. Electroanal. Chem.* **21** (1988) 251
21. B. Wang, J. Tang, F. Wang, *Synth. Met.* **13** (1986) 329
22. S. Wang, F. Wang, X. Ge, *Synth. Met.* **16** (1986) 99
23. Y. Wei, W. Focke, G. Wnek, A. Ray, A. MacDiarmid, *J. Phys. Chem.* **93** (1989) 495
24. J. E. Periera, M. L. A. Temperini, S. I. C. Torresi, *Electrochim. Acta* **44** (1999) 1887
25. J. Lacroix, P. Garcia, J. Audiere, R. Clement, O. Kahn, *New J. Chem.* **14** (1991) 87
26. A. Thyssen, A. Hochfeld, R. Kessel, A. Meyer, J. W. Schultze, *Synth. Met.* **29** (1989) E 357.